

## Chapter II

### Section A

#### Transformative reactions on friedelin

##### 1. Introduction

The discovery of lead for pharmaceutical investigations requires identification of new molecules that are able to interact with and modify a biological target.<sup>29,30</sup> Natural products represent one of the most relevant approaches to this goal. Natural products are produced in living organisms by the activity of biosynthetic enzymes. They are thus recognized by the enzymes at specific binding sites complementary in shape and physicochemical properties. Natural products may possess the imprint for binding to the therapeutic target proteins containing the ligand binding motif similar to the biosynthetic enzyme.<sup>29</sup> Therefore, it is important to identify novel compounds those are complementary to biological structure space.

Triterpenoids are a large, ubiquitous and structurally diverse group of natural products that exhibit nearly 200 diverse skeletons.<sup>31</sup> Most significant triterpenoids are 6-6-6-5 tetracycles, 6-6-6-6-5 pentacycles, or 6-6-6-6-6 pentacycles<sup>32</sup> with physiological functions allied with chemical protection of plants.<sup>33</sup> Triterpenes, highly oxidized at ring A have been reported to possess a wide spectrum of biological activities.<sup>34</sup>

Pentacyclic triterpenes, such as betulinic, boswellic, ursolic, and oleanolic acids are highly abundant in many edible fruits and vegetables. They are reported to inhibit cultured human melanoma, neuroblastoma, malignant brain tumor and leukemic cells.<sup>35,36</sup> They inhibit topoisomerases I and II $\alpha$  by contending with DNA for topoisomerase binding sites, thus preventing topoisomerase-DNA cleavable complex formation.<sup>32,35,36</sup> The general pentacyclic ring structure of triterpenoids has been reported to be essential for topoisomerase inhibitory activity.<sup>37,38</sup> However, the structure itself is inadequate for inhibition and the nature and arrangement of the side groups/functionality are the key factors.<sup>37,38</sup>

Although, friedelan group of triterpenoids are 6-6-6-6-6 pentacycles and are wide spread in nature, surprisingly modern "lead research" on friedelan skeleton is not much

prevalent. In recent times only few works on the transformative reactions on friedelin (1) have been reported.<sup>33,39,40</sup> Some recent studies have indicated the *in vitro* anti-tumor activity of some of hemisynthetic friedelin derivatives,<sup>33,39,40</sup> but the mechanisms through which these compounds achieve this effect has not yet been elucidated. Moreover, the systematic studies on transformative reactions and biological activity of cerin (2) are limited.

## 2. The present investigation

In the present study structurally modified friedelan derivatives, highly oxidized on ring A were synthesised from friedelin (1) and rare cerin (29) and characterized by IR, 1D, 2D-NMR and MS.

### 2.1 Results and Discussion

We have synthesized some hemisynthetic friedelan compounds (59, 59a, 61, 45 and 45a) by simple chemical modifications of triterpenes 1 and 29 (Figure 1) isolated from *Quercus suber* (Cork).

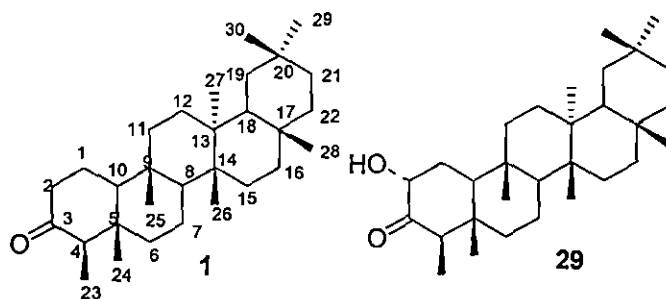


Figure 5 Chemical structures of triterpenoids from *Q. suber*

Two different schemes (Scheme 1 and Scheme 2) were used for their synthesis. Both these schemes are quite suitable for possible large-scale applications. The conversions mainly focused on the oxidative cleavage of the ring A of the natural triterpenoids. The oxidative cleavage of 1 and 29 produced 2,3-secofriedelan-2,3-dioic acid (45) and 4-oxa-3,4-secofriedelan-3-oic acid (59), respectively. A controlled lead tetraacetate (LTA) oxidation on both 59 and 45 at room temperature selectively produced a A-nor-lactone, 61 (Scheme 1 and 2) with 68% yield.

Friedelin, **1** and cerin, **29** were isolated from cork by using soxhlet apparatus. Cerin was obtained as slightly yellowish crystals of melting point (mp) 260-261 °C.

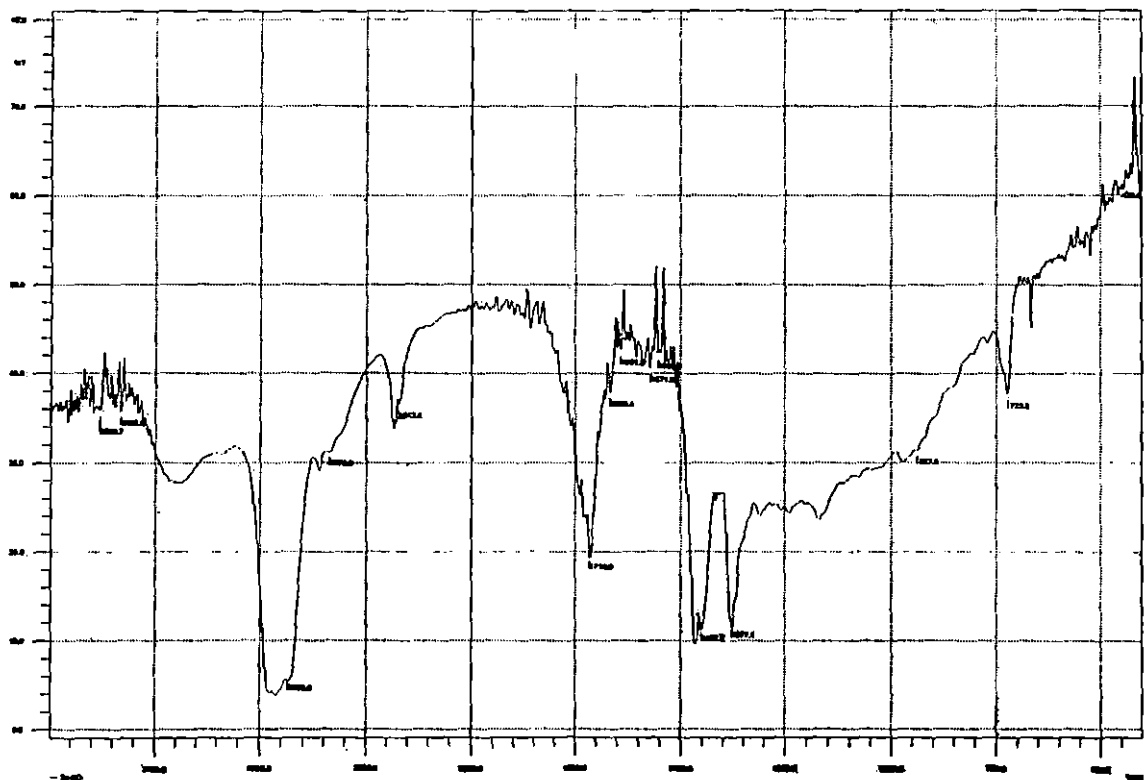


Figure 6 IR spectrum of friedelin, **1**

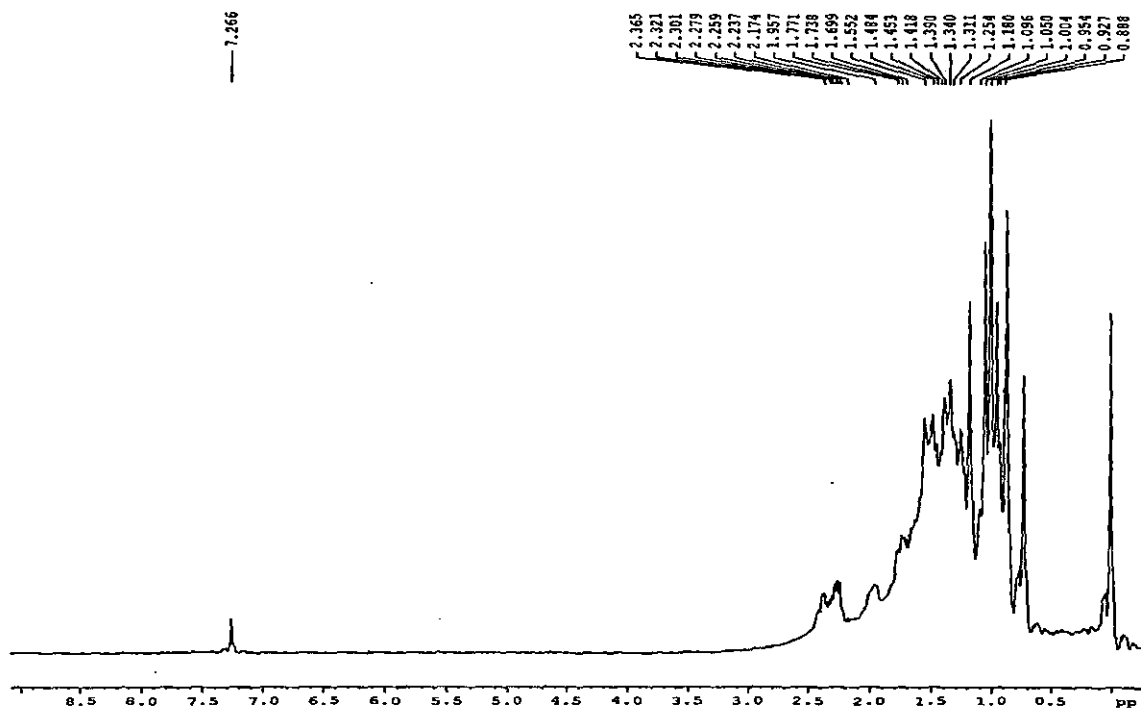


Figure 7  $^1\text{H}$  NMR spectrum of friedelin, 1

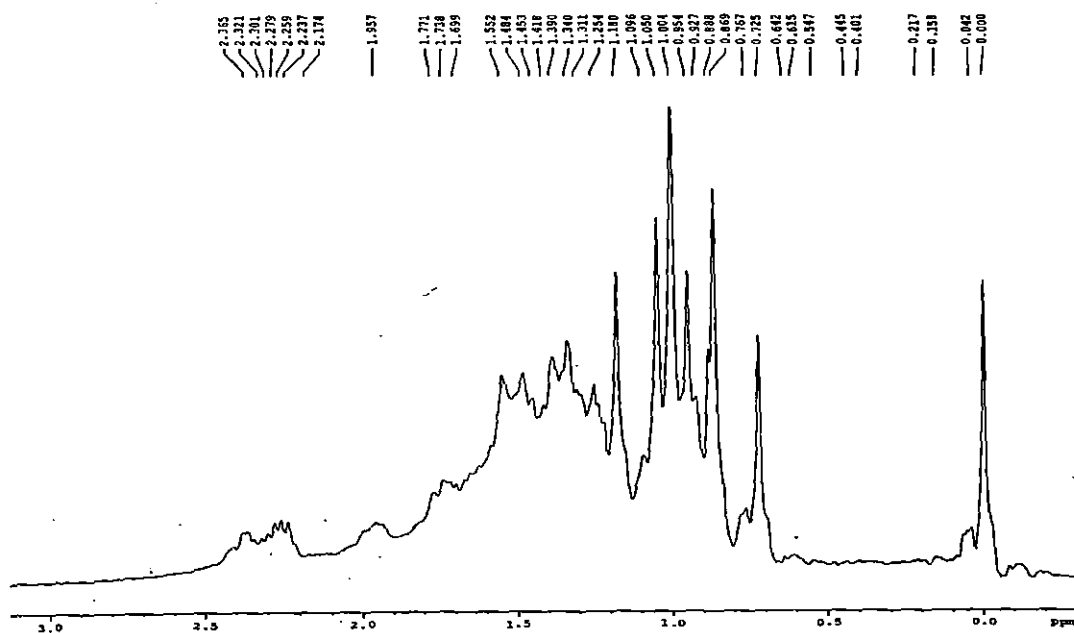


Figure 8 Expanded  $^1\text{H}$  spectrum of friedelin, 1

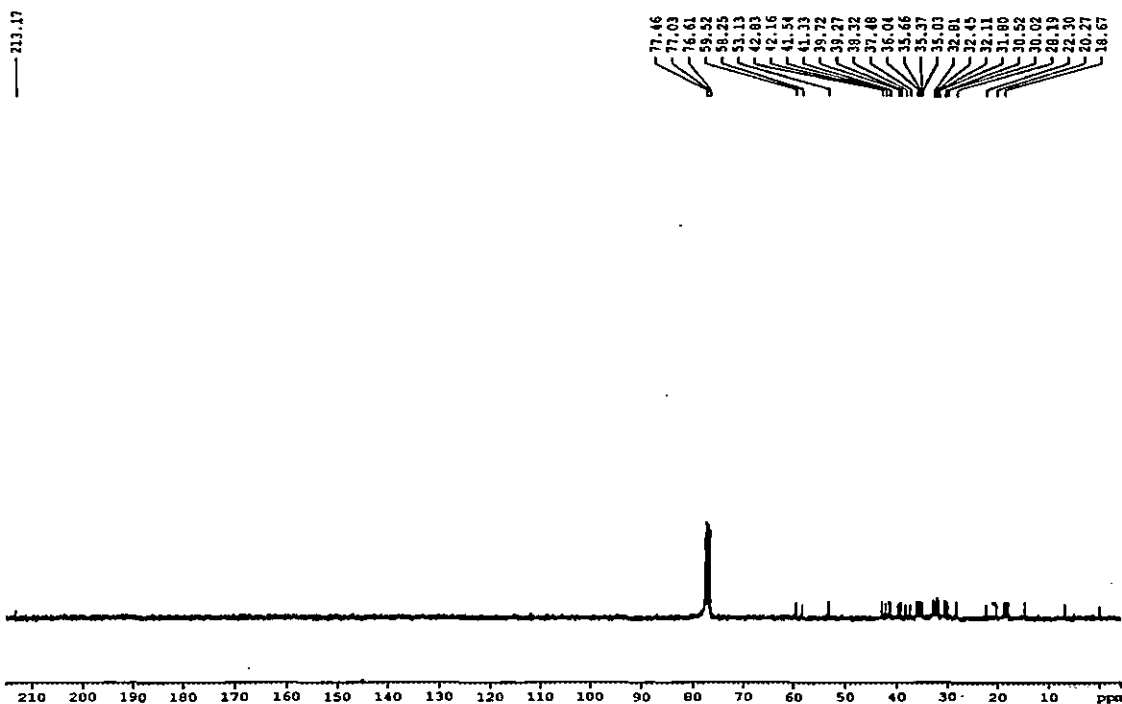
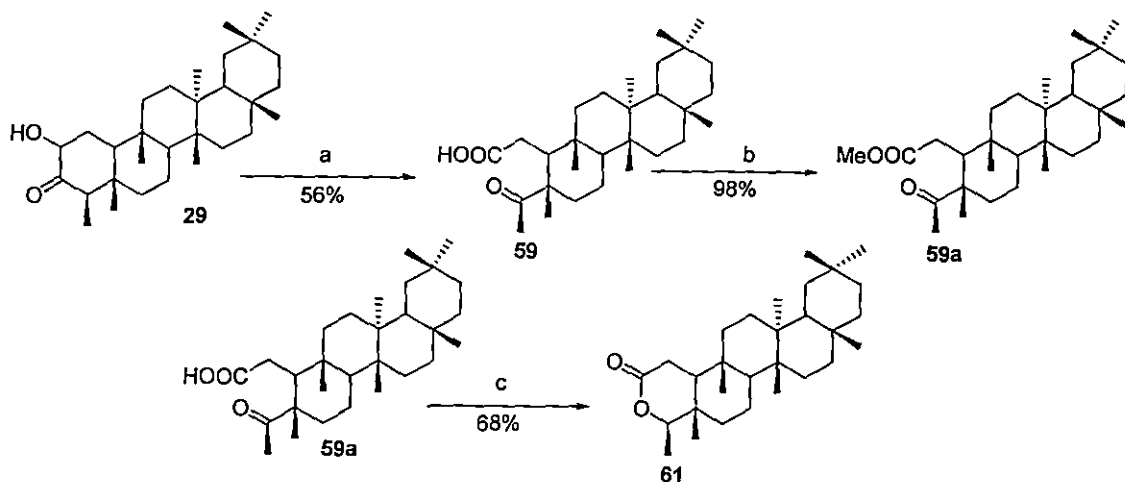


Figure 9  $^{13}\text{C}$  NMR spectrum of friedelin, 1

Oxidation of **29** in glacial acetic acid in presence of anhydrous  $\text{CrO}_3$ , followed by evaporation of the solvent at reduced pressure gave a yellow gummy residue (Scheme 1). Purification of the residue over a column of silica gel gave white powdered compound, **59** of melting point (mp) 214-215  $^\circ\text{C}$ , which upon methylation with diazomethane afforded the corresponding methyl ester **59a** of mp 167-168  $^\circ\text{C}$ . In the IR spectrum compound **59** showed peaks at 3079, 1734 (H-bonded  $>\text{C}=\text{O}$ ), 1696 (carbonyl of COOH group), 1465 (C-O), 1419, 1302, 1074 and 899  $\text{cm}^{-1}$ .  $^1\text{H}$  NMR spectra of compound **59** gave signals for the presence of eight tertiary methyls at  $\delta_{\text{H}}$  0.90 (s, 3H, Me-25), 0.94 (s, 3H, Me-30), 0.99 (s, 3H, Me-26), 1.01 (s, 3H, Me-27), 1.05 (s, 3H, Me-29), 1.13 (s, 3H, Me-24), 1.18 (s, 3H, Me-28) and 2.20 (s, 3H, Me-23). Two methylene hydrogens at  $\text{C}_1$  appeared at  $\delta_{\text{H}}$  1.90 (dd, 1H,  $J_{1\text{eq}10\text{ax}} = 4.0$  Hz,  $J_{\text{gem}} = 15.6$  Hz, H-1) and 2.35 (1H, dd,  $J_{1\text{ax}10\text{ax}} = 6.6$  Hz,  $J_{\text{gem}} = 15.6$  Hz, H-1).  $\text{C}_{10}$  axial hydrogen atom appeared at  $\delta_{\text{H}}$  2.30 (dd, 1H,  $J_{10\text{ax}1\text{eq}} = 4.0$  Hz,  $J_{10\text{ax}1\text{ax}} = 6.6$  Hz, H-10) and the carboxyl hydrogen appeared as a singlet at  $\delta_{\text{H}}$  9.96 (s, 1H, COOH).  $^{13}\text{C}$  spectral data are tabulated in table 1. On the basis of the above data, structure of compound **59** was established as 4-oxa-3,4-secofriedelan-

3-*o*-ic acid. Compound **59** on esterification with diazomethane gave the corresponding ester, **59a** with 94% yield. In its  $^1\text{H}$  NMR spectrum it gave a sharp singlet at  $\delta_{\text{H}}$  3.67 (s, 3H,  $-\text{OCOCH}_3$ ) due to the ester methyl and all other signals were in good correlation to the proposed structure of **59a**. The IR, NMR data of **59** and **59a** were comparable to that reported in literature.<sup>25,26</sup>



**Scheme 15** Oxidative ring cleavage of compound **2**. Reagents and conditions: **a**, Dry  $\text{CrO}_3$ , glacial AcOH, ice cold water,  $\text{CHCl}_3$ , anhyd.  $\text{Al}_2(\text{SO}_4)_3$ ; **b**, Diethyl ether,  $\text{CH}_2\text{N}_2$ , glacial AcOH, ice cold water,  $\text{CHCl}_3$ , anhyd.  $\text{Al}_2(\text{SO}_4)_3$ ; **c**, Lead tetra acetate, glacial AcOH, ice cold water,  $\text{CHCl}_3$ , anhyd.  $\text{Al}_2(\text{SO}_4)_3$

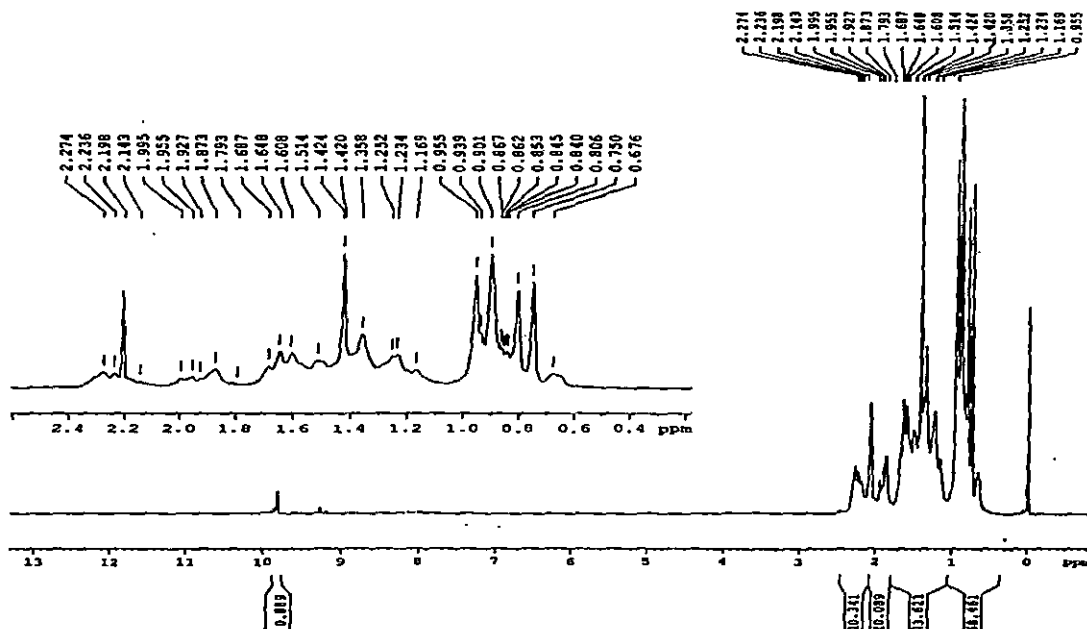


**Figure 10**  $^1\text{H}$  NMR spectrum of compound **59**

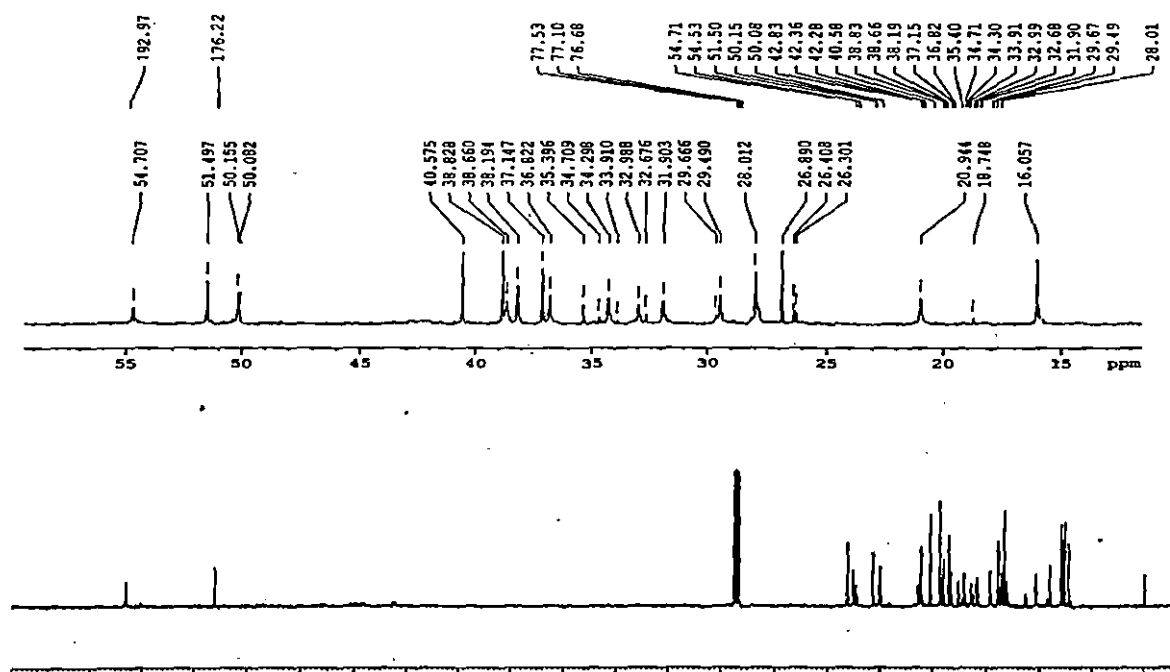
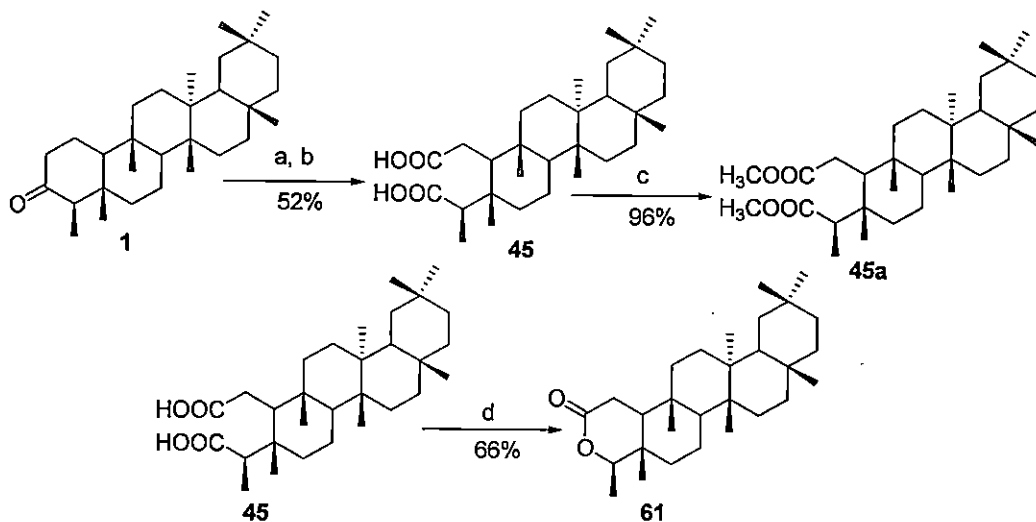


Figure 11  $^{13}\text{C}$  NMR spectrum of compound 59

In another attempt to synthesize friedlan derivatives highly oxidized at ring A, the oxidation of **1** was undertaken with ammonium vanadate in concentrated  $\text{HNO}_3$ -glacial acetic acid at  $0^\circ\text{C}$ . Purification of the reaction mixture through column chromatography yielded a white powdered compound, **45** (Scheme 2). Compound **45a** on esterification by diazomethane yielded the corresponding ester **45a** exclusively of mp  $167$ - $169^\circ\text{C}$ . The IR, MS and NMR (both  $^1\text{H}$  and  $^{13}\text{C}$ ) data of **45** and **45a** were comparable with the data reported in the literature.<sup>23,25,26</sup>



Scheme 2 Oxidative transformation of compound 1. Reagents and conditions: a, Glacial  $\text{CH}_3\text{COOH}$ , Vanadium pentoxide,  $\text{HNO}_3$  cold  $\text{H}_2\text{O}$ , Chloroform,  $\text{Na}_2\text{SO}_4$  (Anhy.); b,  $\text{H}_2\text{O}_2$ ; c,  $\text{CH}_2\text{N}_2$ , dry ether, glacial acetic acid,  $\text{Na}_2\text{SO}_4$  (Anhy.); d, LTA, glacial  $\text{CH}_3\text{COOH}$ ,  $\text{CHCl}_3$ ,  $\text{Na}_2\text{SO}_4$  (Anhy.)

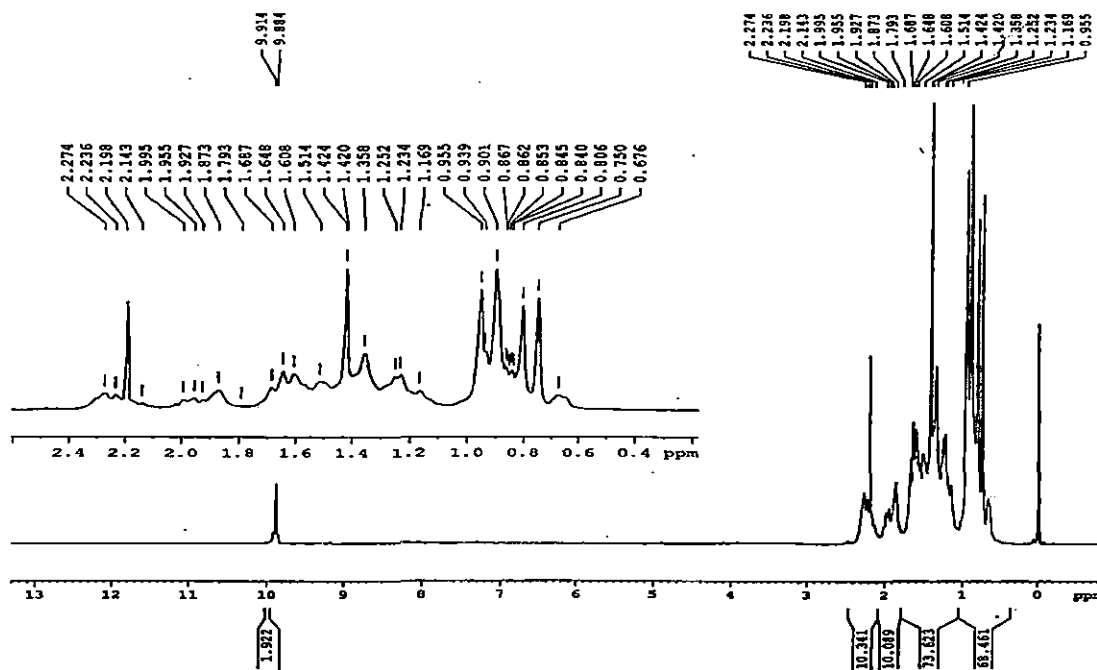


Figure 12  $^1\text{H}$  NMR spectrum of compound 45

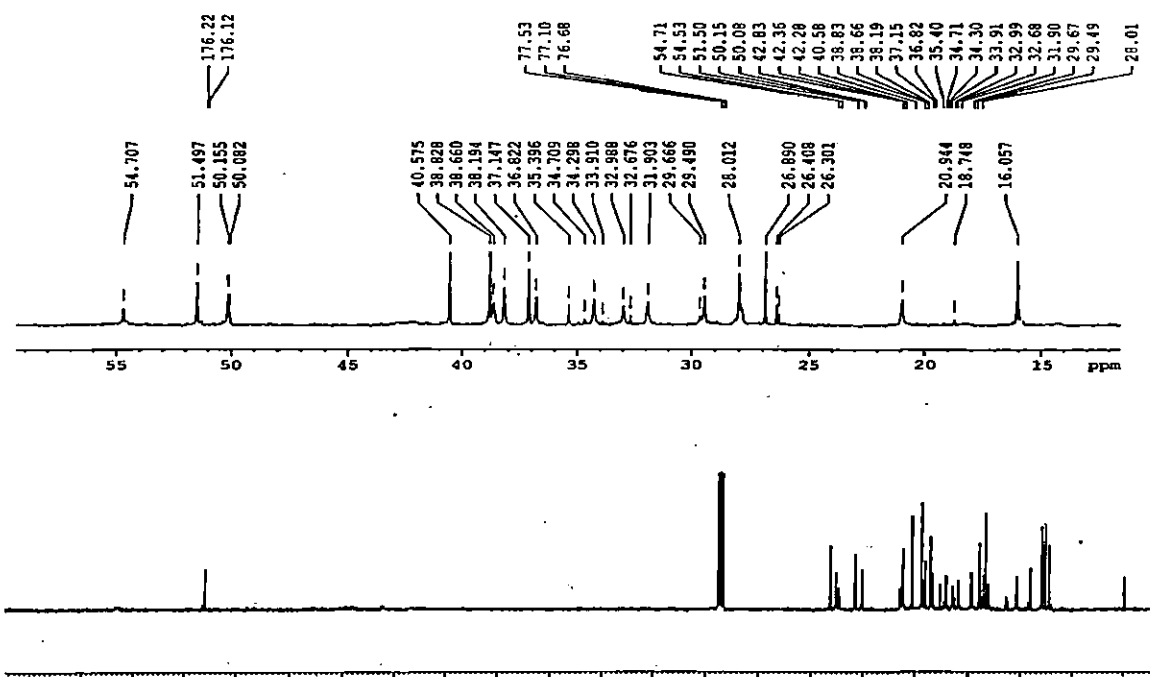


Figure 13  $^{13}\text{C}$  NMR spectrum of compound 45

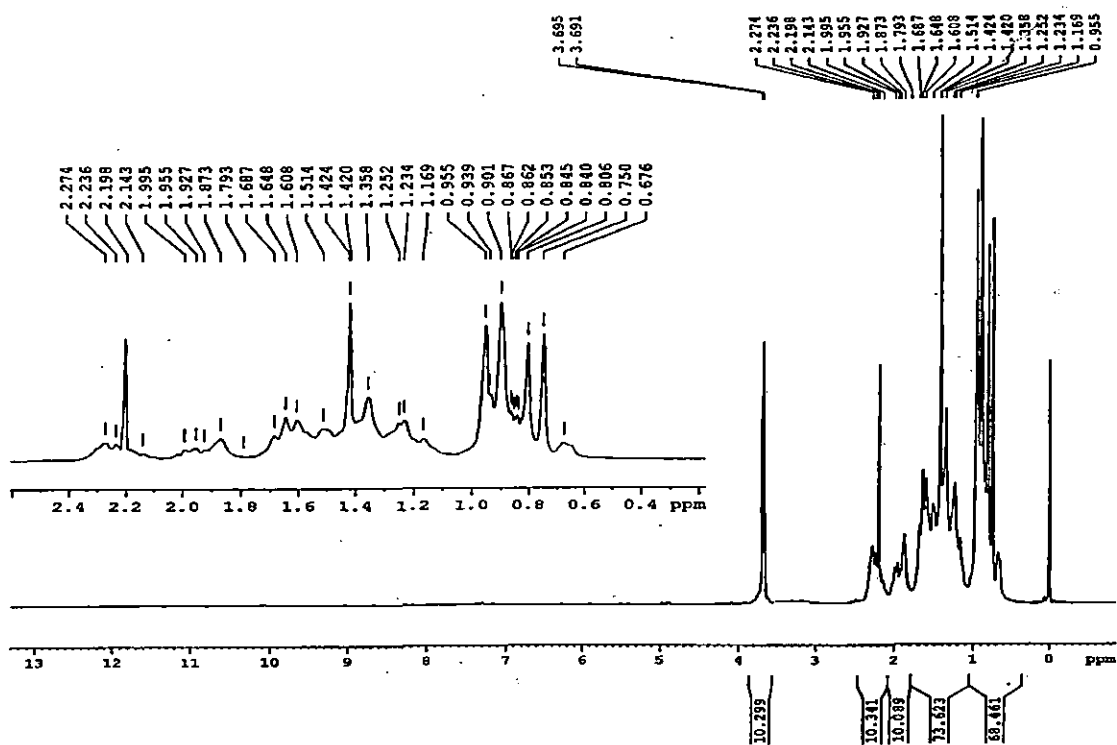


Figure 14  $^1\text{H}$  NMR spectrum of compound 45a

Further oxidation of **59** and **45** separately with LTA in glacial acetic acid furnished the same compound **61**, as white powder of mp 266-267 °C. The molecular formula of the compound, as determined by ESI ( $m/z$  429  $M+1$ ) and TOF ( $m/z$  428  $M^+$ ) MS was  $C_{29}H_{48}O_2$ . This molecular formula was also corroborated by  $^1H$  and  $^{13}C$  NMR spectroscopic data (Table 1). The  $^{13}C$  and DEPT spectroscopic data of **61** revealed the presence of 29 carbon signals including an ester carbonyl ( $\delta_c$  172.1), eight primary, ten secondary, four tertiary and seven quaternary carbon atoms.

The six degrees of unsaturation inherent in the molecular formula of **61**, coupled with the NMR data showed the presence of one carbonyl group and five rings in the molecule **61**. These results indicated that a probable cyclization of the nor-seco acid **59** and seco-diacid **45** had occurred during the LTA oxidation and the nor-lactone, **61** had been generated.

In the IR spectrum, compound **61** gave peaks at 2939, 2866, 1730 (six membered lactone), 1459 (C-O), 1388 (CH-CH<sub>3</sub>), 1241 and 1082  $cm^{-1}$ . In its  $^1H$  NMR spectrum (Figure 10-11) it showed seven tertiary methyl signals at  $\delta_H$  0.84 (s, 3H), 0.89 (s, 3H), 0.94 (s, 3H), 0.99 (s, 3H), 1.01 (s, 3H), 1.06 (s, 3H) and 1.17 (s, 3H, H<sub>3</sub>-28) (Figure 1). Another secondary methyl group at C<sub>4</sub> appeared at  $\delta_H$  1.20 (d, 3H,  $J = 9$  Hz, H<sub>3</sub>-23). C<sub>4</sub>-H appeared as a quartet at  $\delta_H$  4.05 (1H, q,  $J = 6.3$  Hz). C<sub>1</sub>-Hs are deshielded due to the magnetic anisotropy induced by the neighboring carbonyl group at C<sub>2</sub> and each appeared as a doublet of a doublet (dd) centered at  $\delta_H$  2.55 (1H, dd,  $J = 6.6$  and 12.3 Hz,  $\alpha H$ ) and  $\delta_H$  2.40 (1H, dd,  $J = 6.6$  and 12.9 Hz,  $\beta H$ ). The slight difference in the observed 'J' value may be due to the unequal coupling of the axial and equatorial hydrogens on that carbon. H<sub>10</sub> ( $\alpha$ ) appeared as a singlet at  $\delta_H$  1.56 (1H, s). All this data is in good agreement with that for friedelan skeleton.

**Table 1**  $^{13}\text{C}$  NMR data of parent and different hemisynthetic friedelan derivatives

Position	$\delta_{\text{C}}$				
	1	59	61	1*	59*
1	22.3	32.9	34.9	22.3	32.9
2	41.5	176.2	172.0	41.5	178.2
3	213.2			213.3	
4	58.3	193.3	87.6	58.2	233.9
5	42.2	54.7	53.9	42.1	53.4
6	41.3	37.2	39.2	41.3	37.5
7	18.2	18.2	18.6	18.2	17.5
8	53.1	51.5	52.8	53.1	52.5
9	37.5	38.2	37.2	37.4	38.2
10	59.5	50.0	76.6	59.4	49.8
11	35.7	34.3	35.3	35.6	34.4
12	30.5	29.5	30.0	30.5	29.9
13	39.7	40.5	39.7	39.7	39.6
14	38.3	38.6	36.1	38.3	38.3
15	32.5	32.6	32.2	32.4	32.3
16	36.0	35.4	35.8	36.0	35.9
17	30.0	29.7	29.9	30.0	29.9
18	42.8	50.1	42.7	42.7	48.8
19	35.4	36.8	35.0	35.3	35.8
20	28.2	28.0	28.1	28.1	28.1
21	32.8	31.9	32.7	32.7	32.8
22	39.3	38.9	38.1	39.2	39.2
23	6.8	25.3	16.6	6.8	25.3
24	14.7	26.8	12.4	14.6	17.6
25	18.0	18.7	17.5	17.9	17.8
26	20.2	16.1	20.7	20.2	20.2
27	18.7	20.9	16.6	18.6	18.7
28	32.1	33.9	32.1	32.1	32.2
29	35.0	34.7	34.1	35.0	34.9
30	31.8	31.7	31.8	31.7	31.8

\* Reported data in literature

The COSY, NOESY and HMBC spectra (Figure 13-24) of **61** allowed assignment of all the proton and carbon signals. All the  $^{13}\text{C}$  data is presented in table 1. All the above evidence supports the final compound as a nor-lactone. The probability of formation of the other possible six membered lactone (2-oxafriedelan-3-one) was ruled out because of the greater deshielding nature of  $\text{H}_4$  ( $\delta_{\text{H}}$  4.05, 1H, q,  $J = 6.3$  Hz). Nevertheless as compound **61** had been formed from a 2,3-seco compound (either **59** or **45**), there remains every possibility that the stereochemistry at  $\text{C}_4$  had been changed, which may

give rise to structure II (Figure 2). Thus, the probable structures of the compound are either I or II (Figure 2).

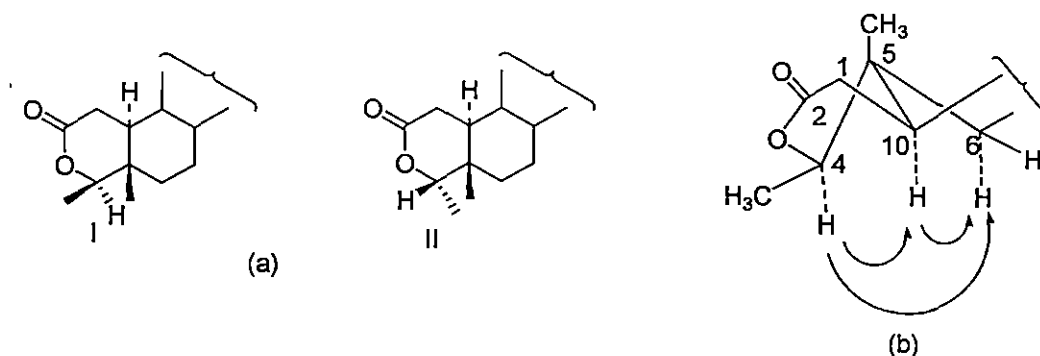


Figure 16 (a) Partial structures of the two possible lactones; (b) Key NOESY correlation of compound **61**

The exact stereochemistry at C<sub>4</sub> was confirmed by 2D NMR techniques. The NOESY spectrum (Figure 19 and 20) of compound **61** gave significant information to this end. All NOE cross peaks have opposite phase to the diagonal, indicating that these arose from positive NOE enhancement as anticipated for a molecule of the size (having M<sup>+</sup> 428) under ambient conditions. In the NOESY spectrum, H<sub>4</sub> at  $\delta_{\text{H}}$  4.05 (1H, q, J = 6.3 Hz) showed two important correlations between H<sub>10</sub> at  $\delta_{\text{H}}$  1.56 (1H, s) and H<sub>6</sub> ( $\alpha$ )  $\delta_{\text{H}}$  1.09 (1H, m). In addition, cross peaks were observed by the NOE effects due to H<sub>10</sub> at  $\delta_{\text{H}}$  1.56 (1H, s) with H<sub>6</sub> ( $\alpha$ )  $\delta_{\text{H}}$  1.09 (1H, m). The above data established the stereochemistry of C<sub>4</sub>-H as alpha and hence structure I (Figure 2) is the exact structure of **61**. Thus compound **61** is 3-oxafriedelan-2-one.

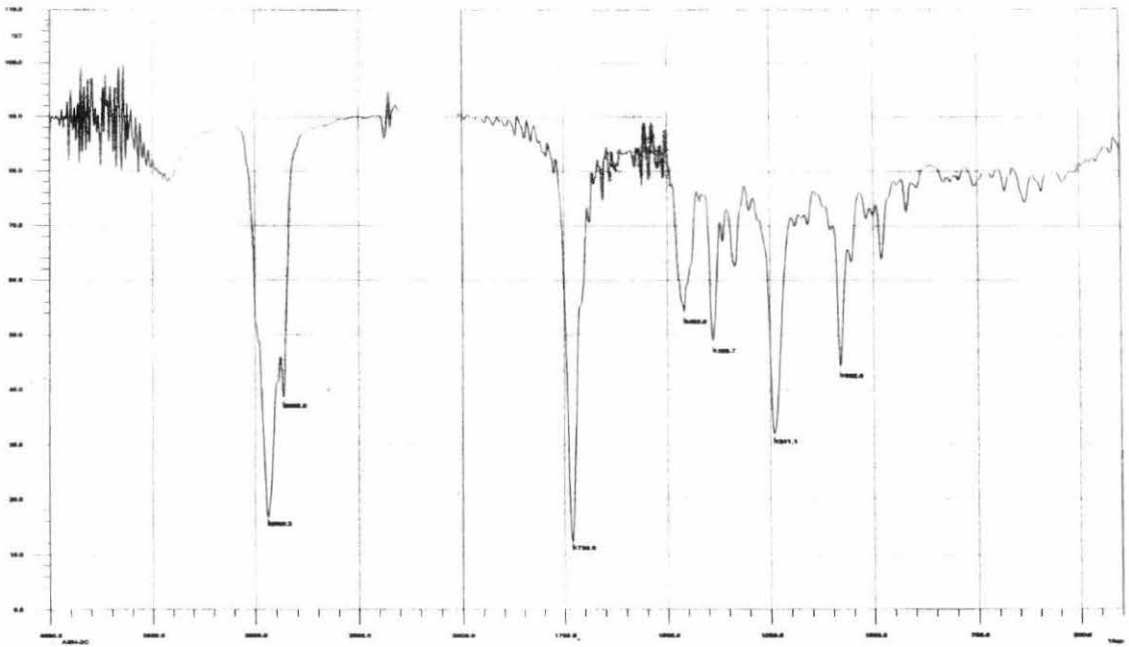


Figure 17 IR spectrum of compound 61

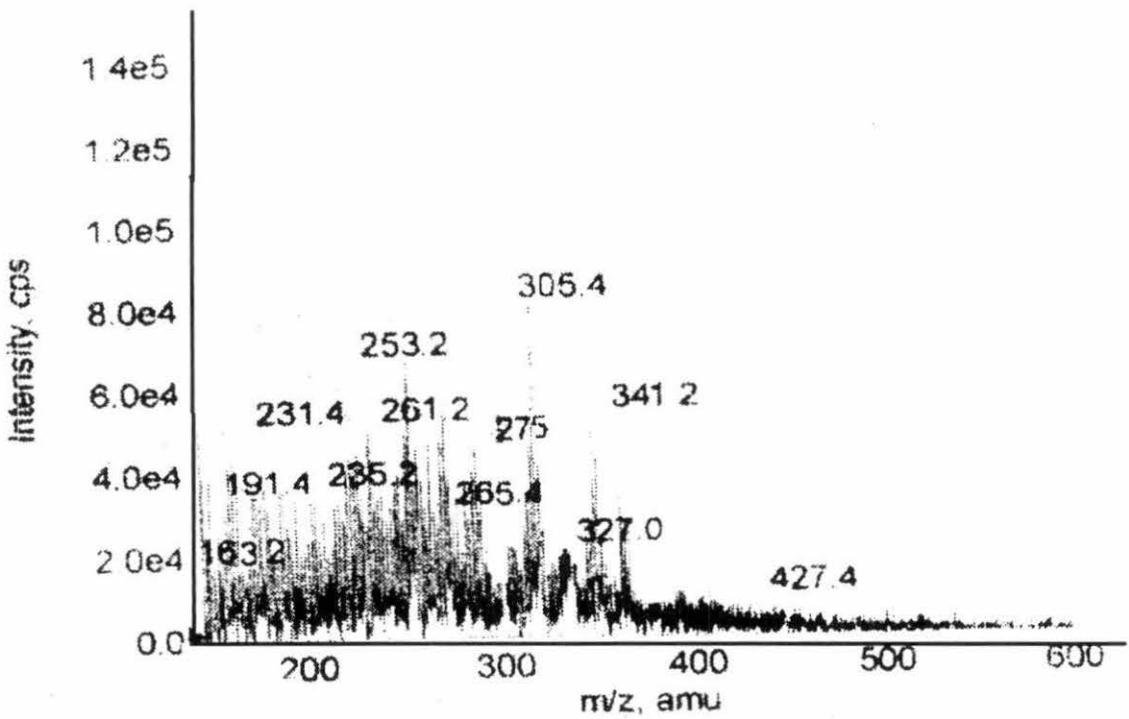


Figure 18 Mass spectrum (ESIMS) of compound 61

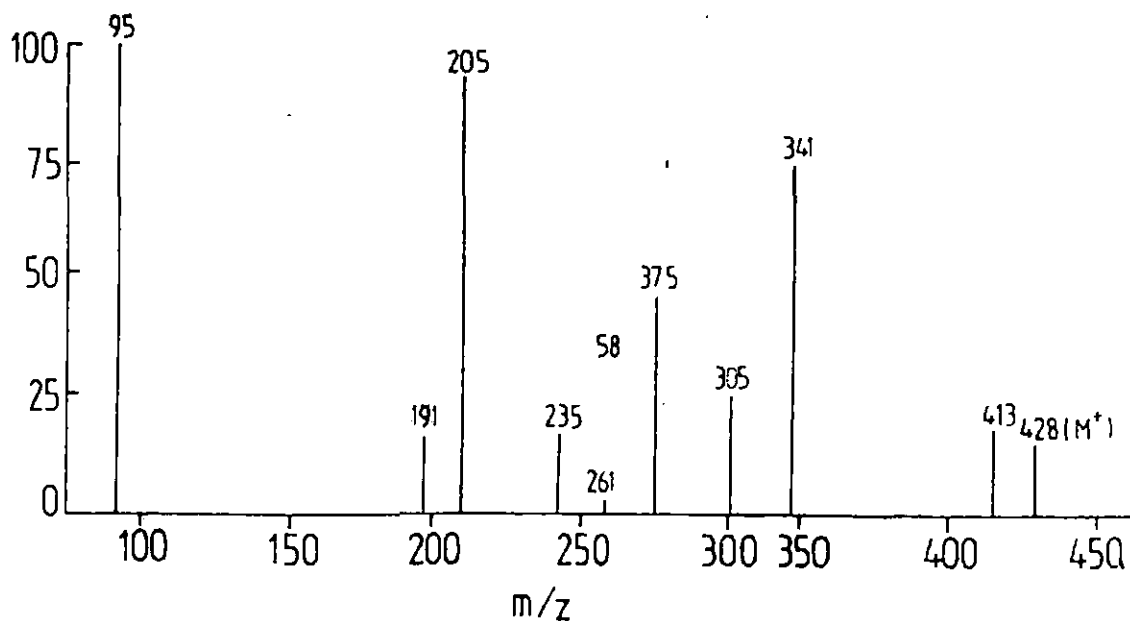
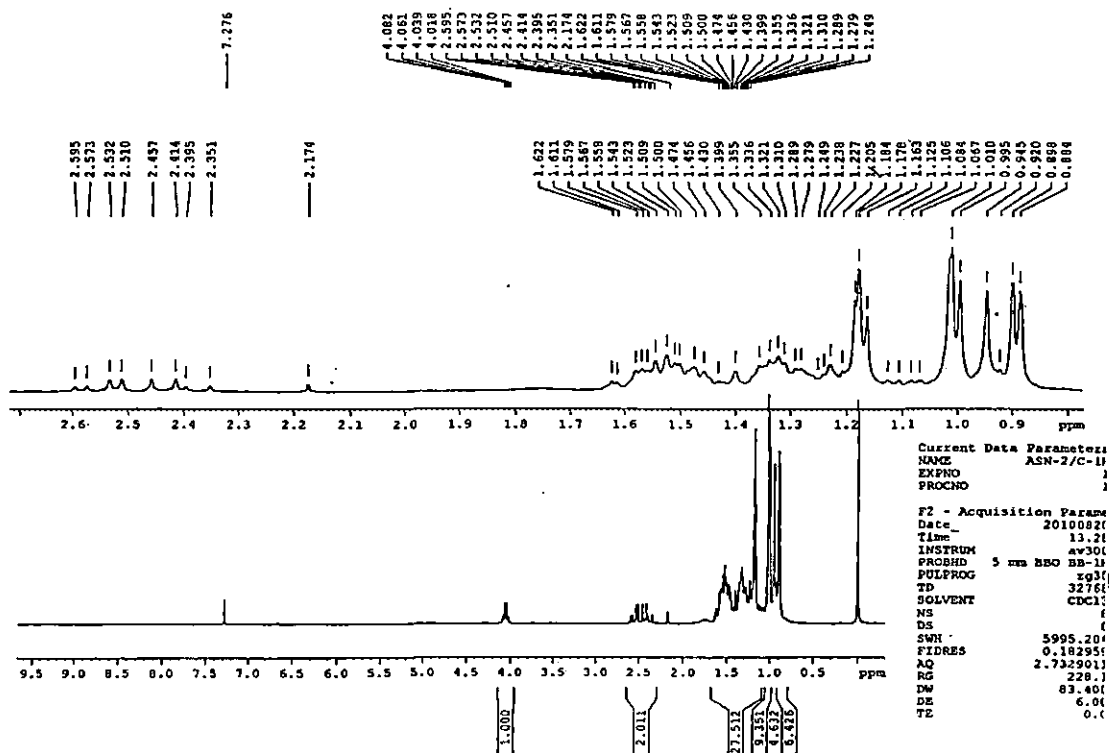


Figure 19 ToF MS spectrum of compound 61



```

Current Data Parameters
NAME      ASN-2/C-11
EXPNO    1
PROCNO   1

F2 - Acquisition Parameters
Date_    20100821
Time     13.21
INSTRUM  av301
PROBHD   5 mm BBO BB-11
PULPROG  zg31
TD       32768
SOLVENT  CDCl3
NS       4
DS       1
SWH      5995.204
FIDRES   0.182955
AQ       2.7329011
RG       228.1
DM       83.401
DE       6.01
TE       0.1
  
```

Figure 20 <sup>1</sup>H NMR spectrum of compound 61

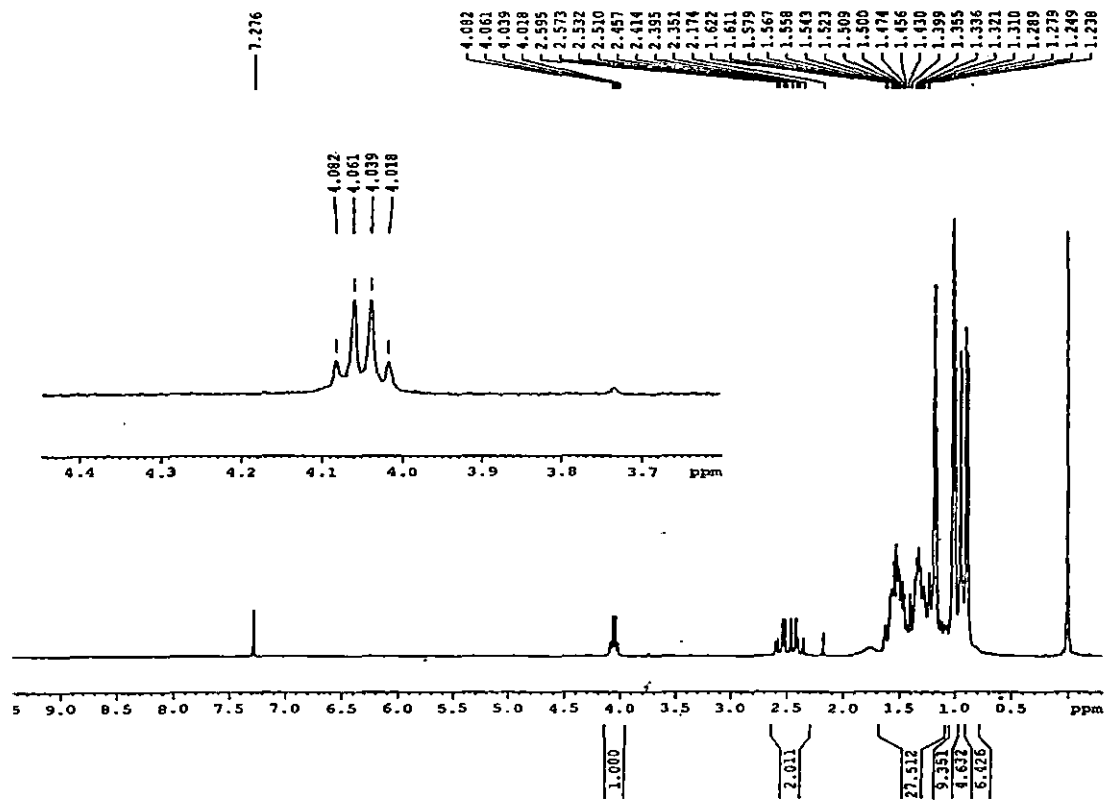


Figure 21 Expanded  $^1\text{H}$  NMR spectrum of compound 61

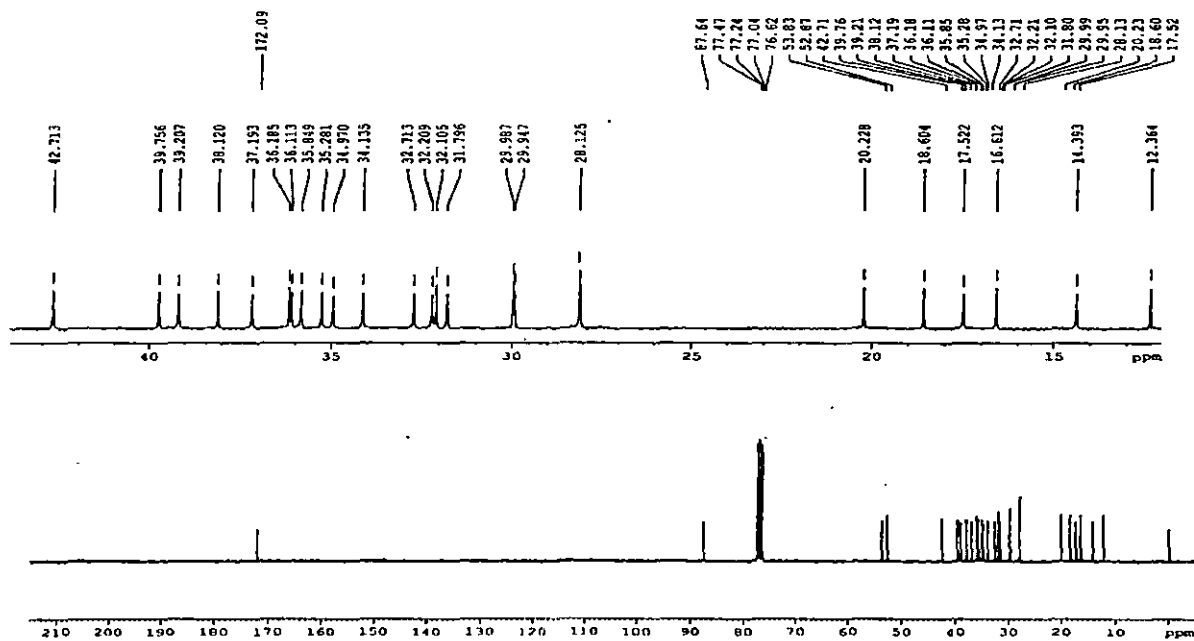


Figure 22  $^{13}\text{C}$  NMR spectrum of compound 61

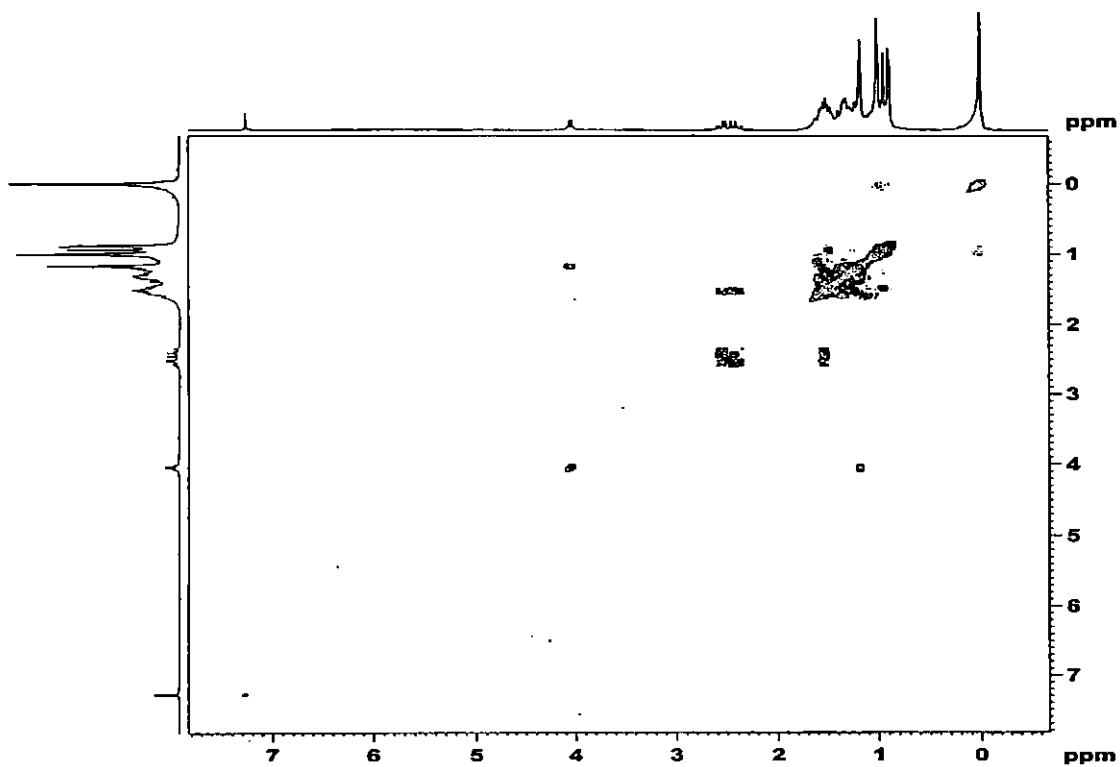


Figure 23 COSY spectrum of compound 61

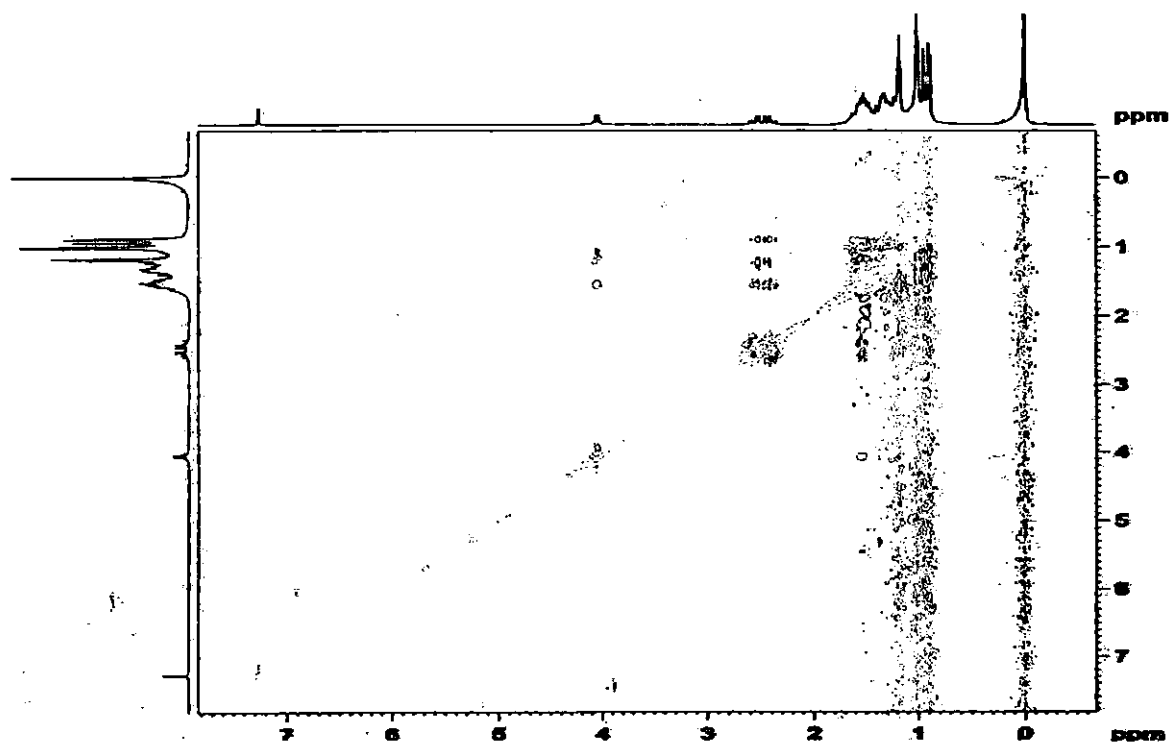


Figure 24 ROESY spectrum of compound 61

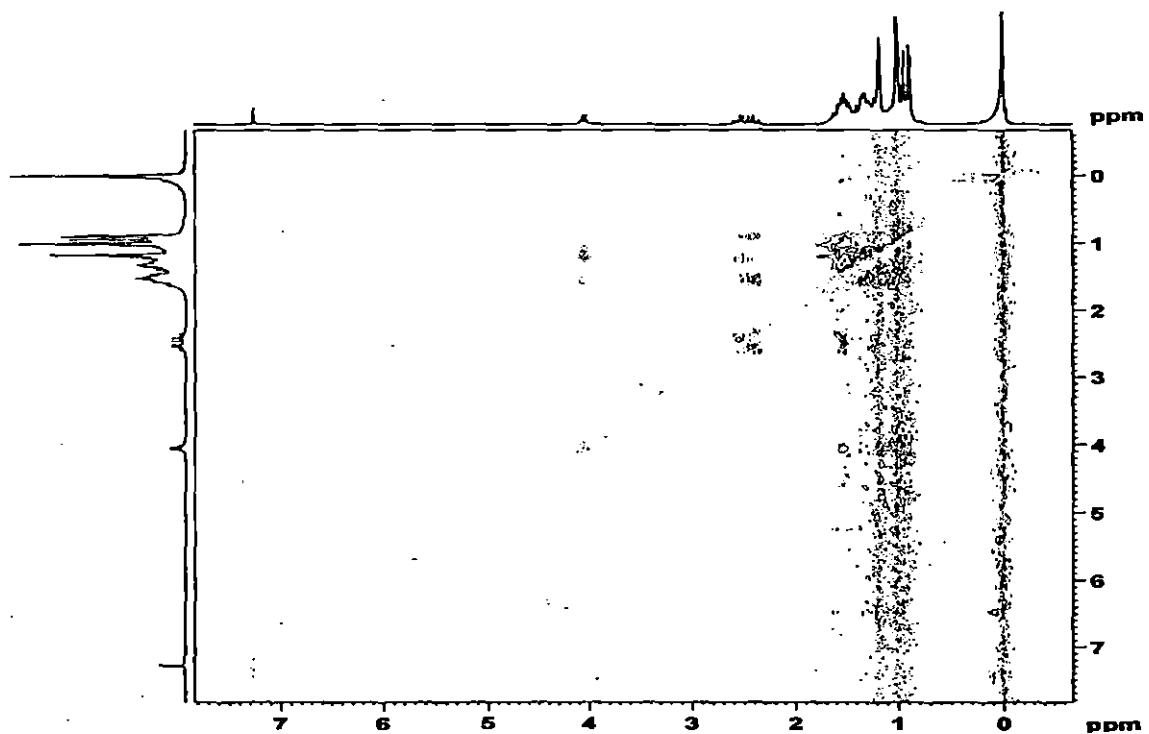


Figure 25 NOESY spectrum of compound 61

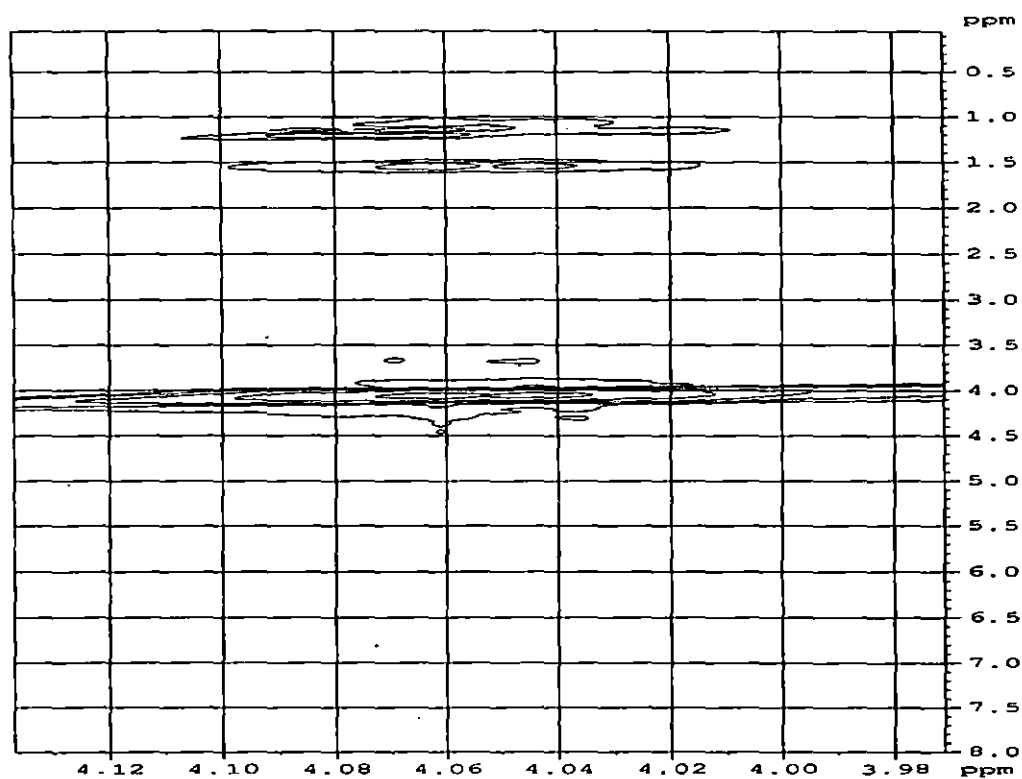


Figure 26 Expanded NOESY spectrum of compound 61

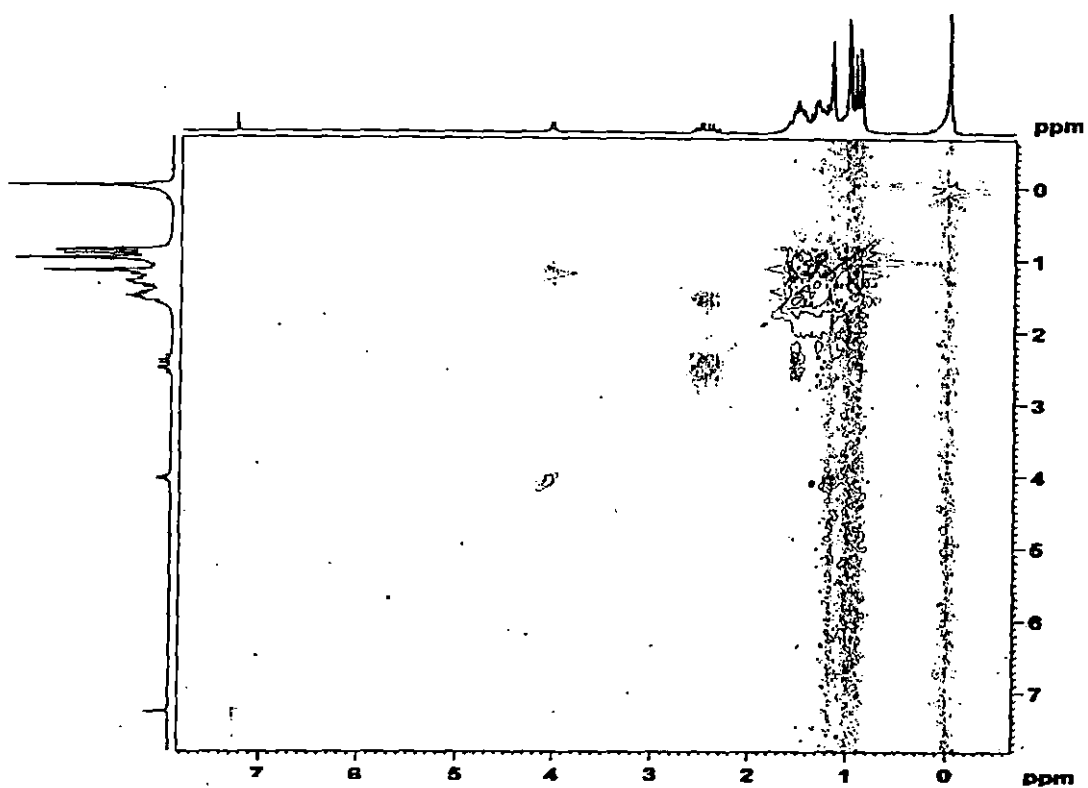


Figure 27 TCOSY spectrum of compound 61

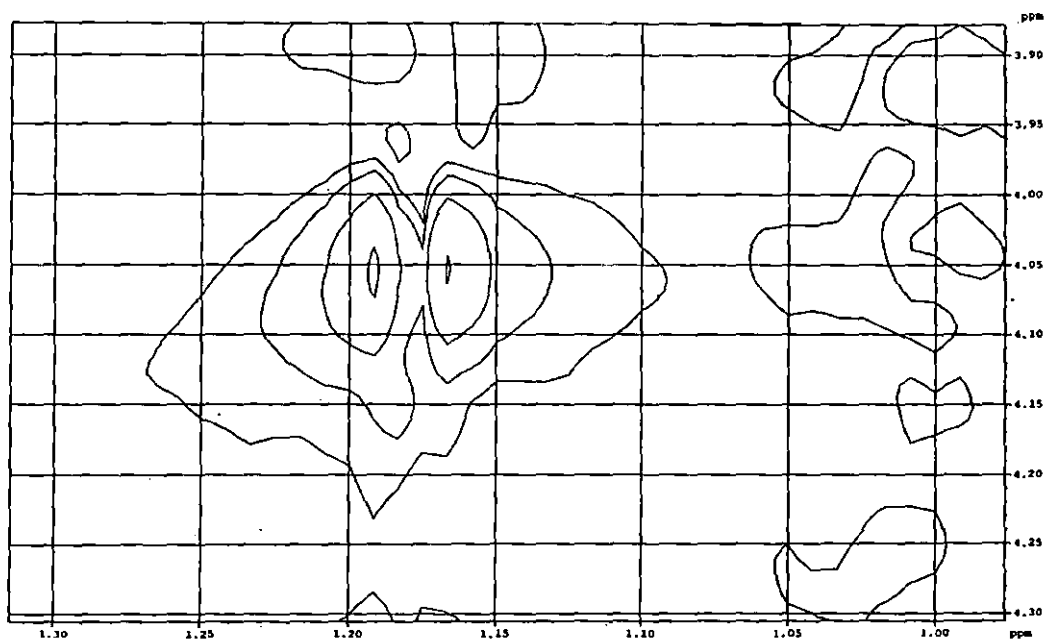


Figure 28 Expanded TCOSY spectrum of compound 61

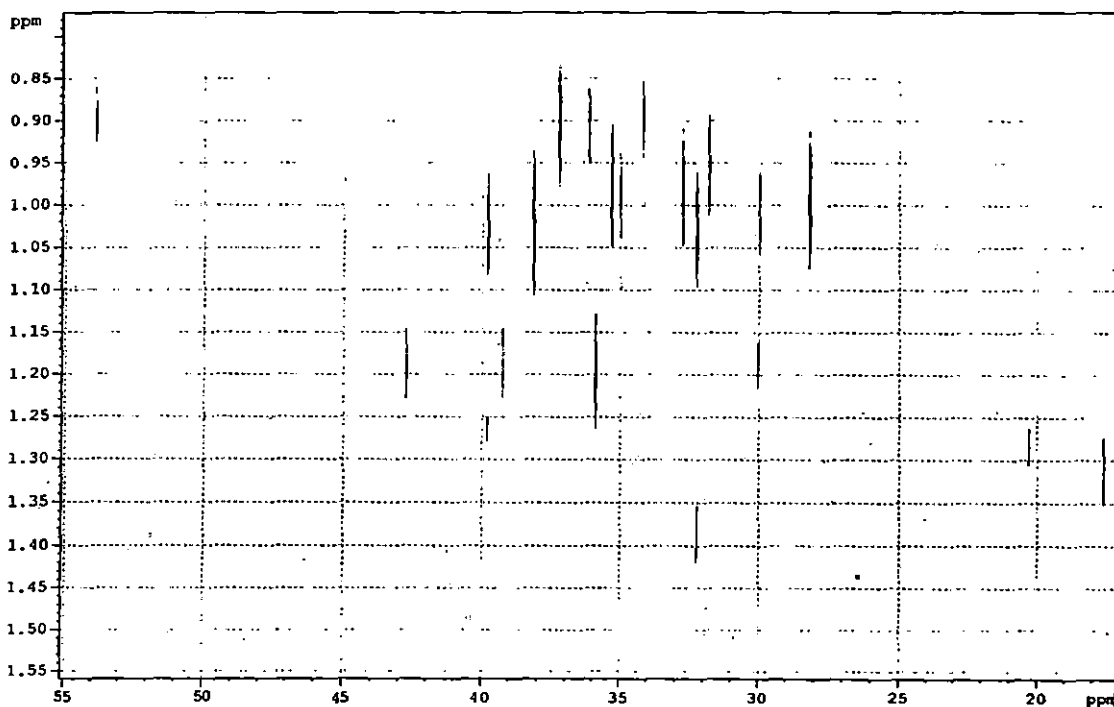
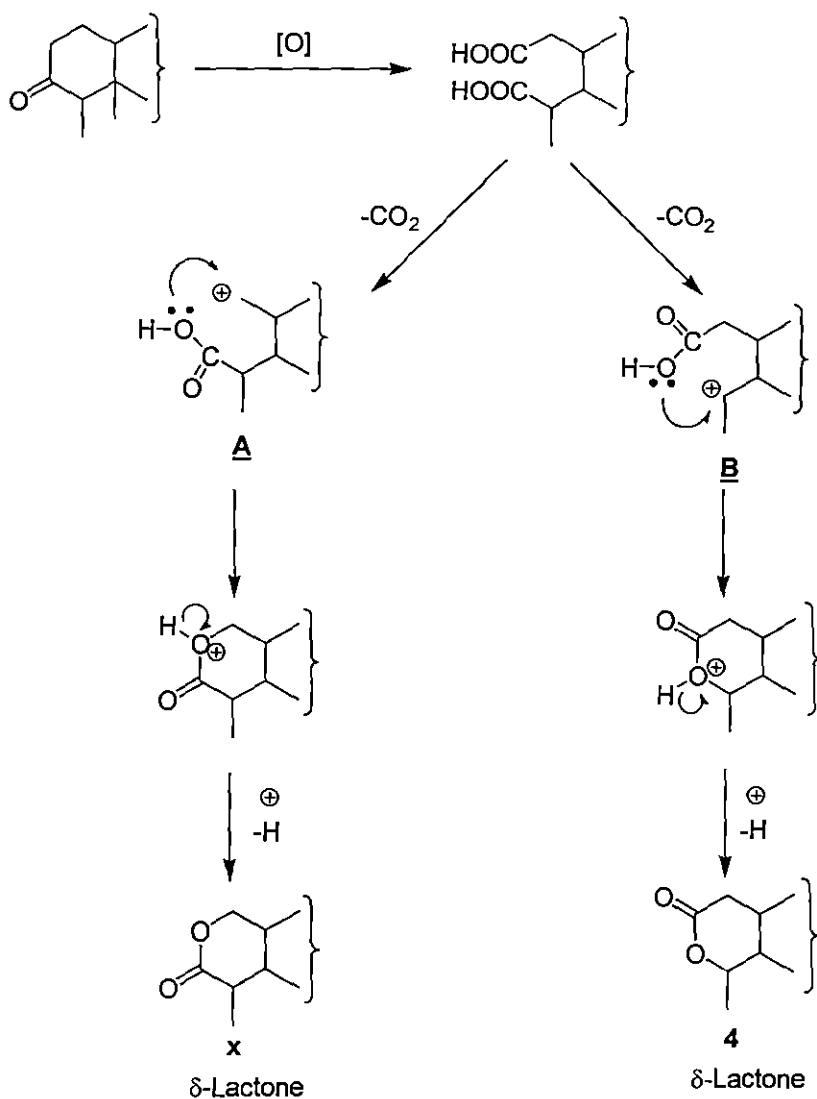


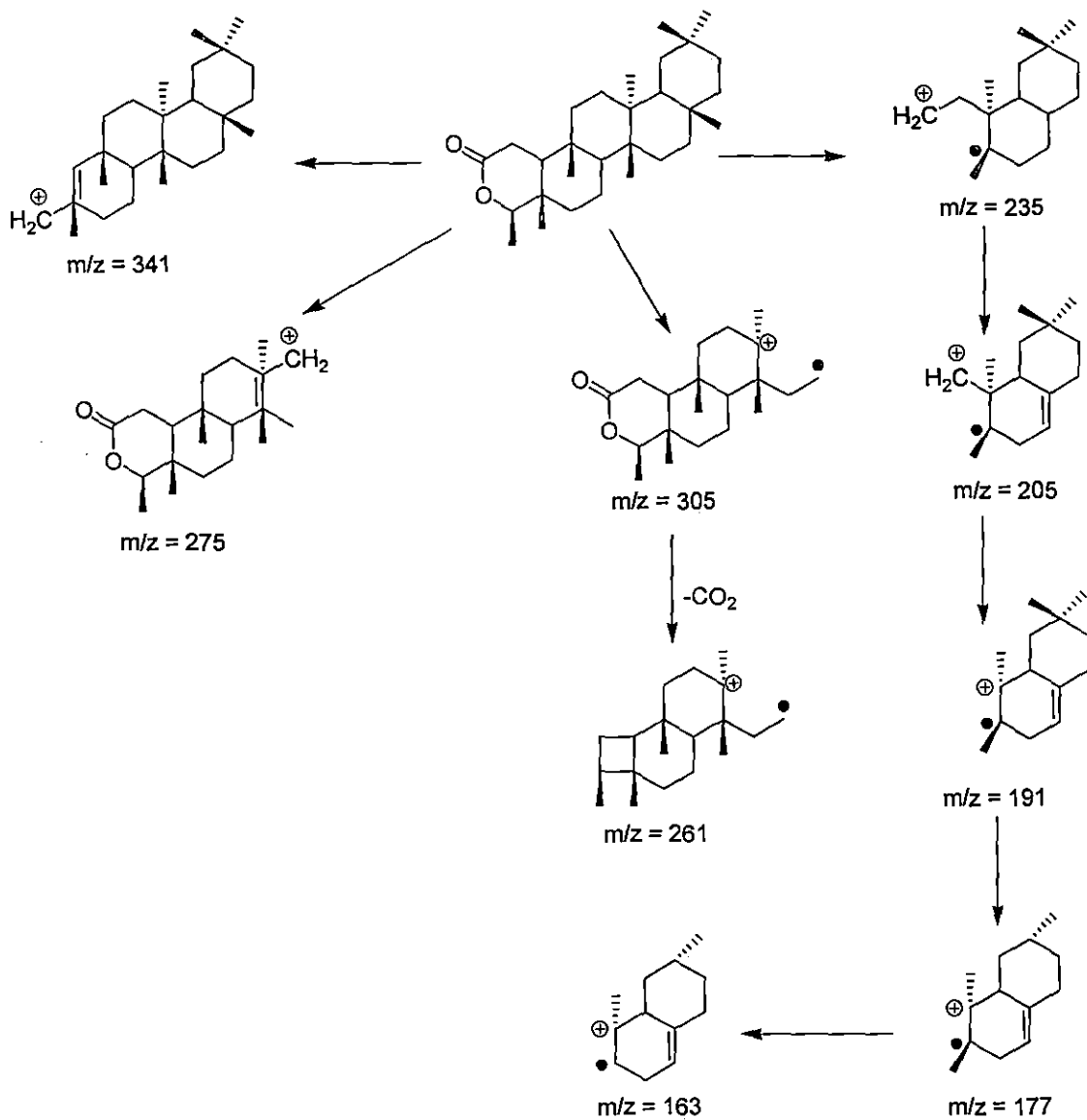
Figure 29 HETCOR spectrum of compound 61

The present author also predicted the mechanism of formation of the  $\delta$ -lactone. It is depicted below. While LTA oxidation, decarboxylation will occur from either of the two positions to generate the carbocation intermediate A or B. Subsequent attack on the carbon site of the cation by the lone pair of electrons on the oxygen atom hydroxyl group of the retained carboxyl acid moiety followed by proton elimination resulted in the formation of two different isomeric  $\delta$ -lactones. However, in practice compound **61** was solely generated. This fact can also be explained by considering the stability of the intermediated carbocations A and B. Being secondary in character, B was more stable than A (a primary carbocation) and therefore, in the reaction medium carbocation had generated exclusively thus forming **61** as the final product of the reaction.



**Scheme 17** Probable mechanism of formation of the  $\delta$ -lactone

Finally the structure of the synthesized  $\delta$ -lactone, **61** was confirmed by the mass fragmentation pattern, schematically represented below (Scheme 18).



**Scheme 18** Probable mass fragmentation pattern of the synthesized  $\delta$ -lactone, 61